The International Journal of Advanced Manufacturing Technology (2025) 141:5271–5288
https://doi.org/10.1007/s00170-025-16893-x

ORIGINAL ARTICLE

Use of a tolerance analysis model for damage identification in structures

Antonio Armillotta[1]

Received: 8 May 2025 / Accepted: 24 October 2025 / Published online: 19 November 2025

Abstract
The paper describes a method for detecting damage in members of a structure from displacement measurements at its nodes. In the context of structural health monitoring, this task is often addressed with model-based methods that compare measurements with values predicted by finite element analysis. In the proposed approach, the underlying model for damage detection is a sensitivity matrix of the same type that is also used in tolerance analysis of mechanical assemblies. The matrix is calculated using the static analogy, a previously proposed tolerance analysis method that has proven particularly useful and straightforward for structures. If statistically abnormal values of the node displacements are detected, their source is localized by a diagnostic test based on the sensitivity matrix. This was validated by means of simulation plans on examples of statically determinate plane trusses. The results help understand how the accuracy of the test depends on the magnitude of the damage relative to measurement errors. Moreover, they suggest that the test can retain an acceptable accuracy even with a significantly reduced subset of measured displacements.

Keywords Structural health monitoring · Damage detection · Tolerancing · Variation simulation · Tolerance stackup

1 Introduction

In the design of mechanical assemblies, tolerance analysis [1–3] verifies that a set of tolerances specified on individual parts satisfies some precision requirements at assembly level. In engineering practice, the task is usually performed with simple charting procedures from direct inspection of technical drawings [4, 5]. Several methods have been proposed in literature [6, 7] to address more complex cases, often with the help of CAD-based software tools.

The core of any tolerance analysis method is a model that calculates an assembly deviation of interest from a given set of tolerance-limited part deviations. A popular type is the linearized model, where the assembly deviation is a sum of part deviations multiplied by appropriate coefficients called sensitivities.

In principle, the stackup model could be used to address an inverse problem. Let the sensitivities be known for a set of assembly deviations, not necessarily associated with functional requirements. If these deviations are measured on a physical assembly, the collected data can be entered as known terms in the linear equations of part deviations. In the event of abnormal assembly deviations, the system of equations can help identify possible drifts on part deviations, which may be associated with damage (e.g. mechanical failure).

Structural health monitoring is a potentially interesting application for this concept. Sensors are often installed on civil or industrial structures to allow the detection of anomalies and implementation of consequent maintenance actions. Specifically, displacement sensors might be placed at the nodes of a structure in order to measure a set of assembly deviations. In the case of abnormal node displacements, the sensitivities could help detect their sources, localizing a possible damage in one of the members of the structure.

This work aims to discuss the feasibility of the diagnostic use of a tolerance analysis model. The reference case addressed is the monitoring of a simple type of structure, namely the statically determinate plane truss. The proposed method is described starting from the underlying tolerance analysis model and showing how it can be integrated into a test for damage detection and localization. The accuracy

✉ Antonio Armillotta
antonio.armillotta@polimi.it

[1] Dipartimento Di Meccanica, Politecnico Di Milano, Via La Masa 1, 20156 Milan, Italy

of the test is evaluated by simulation on some examples, in order to estimate the expected probability of correct damage identification.

The method is demonstrated using a specific tolerance analysis model, which was previously proposed for applications on both structures and generic assemblies. The model is based on a static analogy, which calculates sensitivities through the analysis of forces on an equivalent static model. The paper argues that this choice is justified by the streamlined workflow it offers and its ease of extension to more complex structures. However, the logical distinction between calculating sensitivities and using them for the monitoring task makes the method compatible with most other available models.

The remainder of the paper begins with a recall of related literature on tolerance analysis and structural health monitoring (Section 2) and with a formal definition of the problem (Section 3). The proposed method is then described (Section 4), demonstrated on examples (Section 5), and discussed regarding possible advantages and limitations (Section 6).

2 Related work

This work proposes an application of tolerance analysis in the context of structural health monitoring. In the following subsections, this approach is compared with the state of the art in three stages:

1) The main types of methods for tolerance analysis are recalled and the choice of the proposed method (static analogy) is justified with respect to them.
2) The literature on structural health monitoring is reviewed with a focus on the problem of damage identification.
3) Tolerance analysis is related to a particular category of damage identification methods.

2.1 Tolerance analysis

Tolerance analysis has been studied under a variety of assumptions about the properties of parts and assemblies. This work uses concepts and methods developed for rigid parts in iso-constrained assemblies. Parts are in contact with each other through features with usually simple shapes; these have been classified in textbooks [8, 9] and technical standards [10], which discuss their kinematic properties and typical combinations. Design tolerances are specified on part features to limit random deviations from nominal geometry due to inaccuracies in manufacturing processes.

Due to contact relations, part deviations stack up causing deviations on the geometry of the assembly. In any method of tolerance analysis, a mathematical model is built to compute an assembly deviation (chosen for its functional relevance, e.g. a gap between two parts) from a given set of part deviations. The available models correspond to different ways of representing geometric transformations between deviations of different types (linear, angular) combined in the typical patterns associated with different types of features (flat, cylindrical, prismatic, etc.), taking into account the kinematic degrees of freedom constrained by the relations (contacts or fits). Transformations are expressed as operations on suitable mathematical entities, which include the following (citing only a small sample of the main references):

- homogeneous matrices, as in the variational model [11–13] and in the matrix model [14, 15];
- position vectors, as in the vector loop model [16–18];
- vectors of screw parameters, as in the small displacement torsor model [19, 20];
- Jacobian matrices, as in the Jacobian model [21], in the Jacobian-torsor model [22–24], and in some extensions of the latter to deal with overconstrained assemblies [25, 26];
- convex volumes of displacements, as in the T-maps model [27, 28], in the deviation domain model [29, 30] and in other convex-hull models [31, 32];
- perturbed meshes, as in the skin model shapes methods [33–36].

These models are either implemented as procedural scripts or automatically built with the help of CAD-based software for variation simulation. In either case, they allow to simulate the effects of combinations of part deviations allowed by the design tolerances. The simulation consists of repeatedly running the stackup model on instances of random part deviations sampled from appropriate statistical distributions, e.g. [37]. The distribution of the assembly deviation is estimated from the results of the simulation runs using the Monte Carlo method [38, 39] or reportedly more efficient quasi-Monte Carlo methods [40–42].

In tolerancing practice, a simple expression of the stackup model is usually deemed useful. Linear equations are especially convenient yet accurate enough because of the small magnitude of deviations: the coefficients of such equations are the sensitivities of the assembly deviation with respect to the part deviations. Most of the above cited models are nonlinear and do not show the explicit contribution of part deviations to the assembly deviation. However, they can be linearized through simulation plans with finite differences of the input tolerances [43, 44].

Some models allow direct linearization, i.e. the direct calculation of sensitivities without the need for repeated simulation runs. The earliest and most popular of these is

the vector loop model mentioned earlier [16–18]. Other models have been modified for the direct calculation of sensitivities; this has been especially required for the models with the highest computational burden, such as convex hull [45, 46] and skin model shapes [47]. In [48], the linearization is done by perturbing parametric geometric models of parts and assemblies, without the need for an underlying stackup model.

A further method of direct linearization, which will be used in this work and recalled in subSection 4.1, is based on a static analogy. The assembly is loaded with an external force corresponding to the assembly deviation of interest, and the sensitivities are calculated by appropriately chosen internal forces on the parts [49, 50]. The approach has also been validated for statically determinate plane trusses [51]. For this special type of assembly, force analysis can be done either manually or with the finite element method (FEM), thus automating the calculation of sensitivities with minimal effort on interactive setup. The workflow is therefore almost as convenient as in the vector loop model, which has also been successfully applied to planar linkages [52, 53].

The use of FEM in tolerance analysis is widespread when dealing with compliant assemblies such as those fabricated by joining sheet metal panels. In that context, the method of influence coefficients (MIC, [54]) calculates sensitivities as deflections of the structure under clamping forces needed to compensate for geometric deviations at the joints. These are calculated from the influence coefficients, i.e. joint displacements caused by unit forces corresponding to part deviations. Later extensions, e.g. [55, 56], and software implementations [57] have allowed to develop and validate the MIC as an invaluable tool for assembly design in the automotive and aerospace sectors. The static analogy has some common aspects with the MIC, such as the application of unit forces to the assembly. As discussed in [58], however, it associates sensitivities to support reactions and internal forces rather than to deflections. This simplifies the calculations on assemblies of rigid parts, while it may be less efficient in handling complex problems of compliant tolerance analysis.

On a wider spectrum of geometric configurations and through simulation plans, the tolerance analysis of structures can be done using more complex methods developed for mechanisms; these include mechanism reliability [59], configuration space [60–63], and extensions of screw theory [64–66].

2.2 Structural health monitoring

Structural health monitoring (SHM) is the use of sensors (as an alternative to visual examination or non-destructive testing techniques) to detect and localize damage on structures [67]. Many damage conditions cause changes in the stiffness of the structure. In many cases, these are monitored through the measurement of vibrations using networks of sensors of different types (accelerometers, strain gauges, fiber-optic or piezo-electric sensors). These have evolved from contact sensors [68] to wireless and smart sensors [69] to embedded sensors [70], allowing an easier integration into structures. Some studies report uses of vibration sensors on truss structures [71–73]. In alternative to vibrations, static displacements have also been measured for the monitoring of truss structures using laser sensors [74] and fiber Bragg grating [75].

A recent trend in SHM is the vision-based measurement of vibrations and static displacements [76, 77]. As discussed in [78–80], this solution has potential advantages such as lower installation cost and ease of collecting measurements at many points in the structure. Current limitations include lower resolution, difficulty in continuous online monitoring, and sensitivity to environmental and lighting conditions. Techniques for extracting displacements from images, such as digital image correlation and motion capture, are compared in [81, 82]. Although applications on trusses are still limited, some studies describe the use of vision-based systems to monitor dynamic responses [83, 84], deflections [80, 85], and static displacements [86] of large structures such as railway bridges and building frames.

The collection of measurements makes it possible to identify abnormal changes, which could be due to damage conditions. As reported in [87], this task includes reporting the occurrence of damage (damage detection) and assigning it to a specific part or substructure (damage localization). Among the algorithms proposed in literature, some use only sequences of measured data (data-driven methods), while others also rely on mathematical models of the undamaged structure (model-based methods).

Data-driven methods generally include a preprocessing step to reduce data dimensionality and extract useful features. These are then used to detect and localize the damage, generally through damage indicators calculated for the applicable sources. As reviewed in [88, 89], principal component analysis and T^2 statistics are the most popular techniques to treat discrete measurements of vibration or static displacement. In [90], vibration measurements are analyzed in the time domain by defining a damage index based on strain energy. More often, they are converted to either the frequency or the modal domain to reduce dimensionality at a compromise with accuracy; specific methods include mode shape curvature [78], modal norms [91], and the output of modal filters in the frequency domain [92]. In other studies, damage indicators are obtained from wavelet transforms [73, 75, 93].

Model-based methods often include a parametric FEM model of the structure, on which the effects of predefined damage modes can be preliminarily calculated. Damage indicators are based on deviations of actual measurements from the predicted effects. Again, the effects are often defined in the frequency domain: natural frequencies are calculated for the different damage modes by directly modifying stiffness matrices [94] or by adding virtual masses to specific members of the structure [95]. The likelihood of each damage mode is then expressed by differences from the corresponding frequencies for the original structure, such as the cosine similarity [96]. Alternatively, the output of the simulation is expressed through the modal parameters that determine the damage indicators by statistical tests [97]. A further approach associates the effects with specific shifts or deflections; these are directly compared with those of the undamaged structure [98] or used to define damage indicators by the method of transmittance functions [99]. In [100] the identification of damage is facilitated by reducing the size of the model by machine learning techniques.

2.3 Objective

The above cited SHM methods have been thoroughly tested on either laboratory testbeds or real facilities, showing their full potential towards the goal of building effective and affordable systems for checking the integrity of critical infrastructures. The present work does not aim to overcome any limitations of these methods, nor to test a specific system of measurement and data processing. Rather, it proposes the concept for a further approach to the damage identification task, that may be used as an alternative to the existing ones in some cases.

The SHM reference case assumes that a vision-based system (or a wireless sensor network) is installed on a structure to measure static displacements at selected points located at the nodes. The goal is to detect and localize damage associated with a dimensional drift in one of the members, which may have caused abnormal node displacements. As in model-based methods, the damage is to be identified by a single set of measurements without the need to analyze sequences or continuous signals. Instead of FEM models, however, the proposed approach uses a tolerance analysis model. This involves a change in the meaning of the variables originally involved in tolerance analysis: part deviations do not come from manufacturing errors, but from drifts due to structural damage (members and joint failures, wear, corrosion, etc.), while assembly deviations correspond to geometric responses measured on the structure.

As will be shown below, a damage identification model based on tolerance analysis can be calculated simultaneously for all possible damage modes without any modification of the static model of the structure. In addition, the expression of the model as a sensitivity matrix allows in principle the calculation of damage indicators through simple inversion, albeit with appropriate modifications to reduce the effect of measurement errors. Finally, the method is potentially compatible with several possible tolerance analysis models as an alternative to the static analogy used in this work.

3 Problem and assumptions

The reference case that will be discussed in the following is a statically determined plane truss of the type shown in Fig. 1. The structure has n_N nodes and $n_M = 2n_N - 3$ bar members. The nodes are of the pin-jointed type, which approximates the behavior of actual joints (e.g. welded, bolted, and riveted) assuming that the loads are applied to nodes. Not excluding other configurations with equivalent constraint, the supports include a hinge and a roller at two different nodes.

The nominal configuration of the truss includes nominal lengths for the n_M members and nominal positions (for a total of 3 coordinates) for the supports. These will be called design dimensions; their number is

$$n = n_M + 3 = 2n_N \tag{1}$$

After the structure is erected, the design dimensions have nominal values x_i ($i = 1, \ldots n$). Later on, some of them may experience deviations δx_i (drifts) due to damage conditions. For a member, the deviation can be due to a change in length or to a shift in one of its end joints. For a support, it can be any displacement in a constrained direction.

The positions of the n_N nodes are each defined by two coordinates (horizontal and vertical), which will be called assembly dimensions. Their number is

$$2n_N = n \tag{2}$$

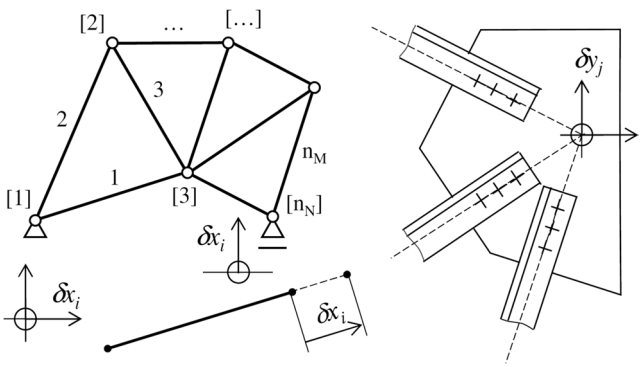

Fig. 1 Drifts and assembly deviations in a plane truss

Assembly dimensions have nominal values y_j ($j=1, \ldots n$) and deviations δy_j. Initially, the y_j are a consequence of the x_i and possible static deformations, e.g. due to dead weight. The δy_j are a consequence of the δx_i and can be measured at any time with appropriate sensors. Each measurement includes the true assembly deviation and a random measurement error.

In a structural monitoring context, the drifts δx_i on design dimensions should be estimated from measured deviations δy_j on assembly dimensions. If one or more design dimensions show excessive drifts from a predefined amount, this may be due to structural anomalies that can be diagnosed and mitigated by appropriate actions (inspection, maintenance, repair).

This goal can be regarded as the inverse problem of tolerance analysis, in which assembly deviations must be estimated from design deviations (usually limited by tolerances specified on individual part dimensions). A common assumption in tolerance analysis methods is that deviations are small relative to part dimensions. It is believed that such a condition applies to common applications in mechanical assemblies, where the coefficient of variation is often of the order of 10^{-3}. For medium-sized structures, this would correspond to drifts within 10–20 mm which are of actual interest for monitoring projects. Sensor readings are likely to be reset to zero on the erected structure so as not to include assembly shifts and static deformations, which might have a greater magnitude.

Under the above assumption, the tolerance analysis can be carried out using the following linear model:

$$\boldsymbol{\delta}\mathrm{y} = \mathrm{S} \bullet \boldsymbol{\delta}\mathrm{x} \tag{3}$$

where $\boldsymbol{\delta x}=[\delta x_1, \ldots \delta x_n]^{\mathrm{T}}$ is the vector of design deviations, $\boldsymbol{\delta y}=[\delta y_1, \ldots \delta y_n]^{\mathrm{T}}$ is the vector of assembly deviations, and

$$\mathbf{S} = \begin{bmatrix} S_{11} & \cdots & S_{1n} \\ \vdots & \ddots & \vdots \\ S_{n1} & \cdots & S_{nn} \end{bmatrix} \tag{4}$$

is the sensitivity matrix, which can be evaluated using one of the available tolerance analysis methods.

The knowledge of **S** is also useful for the above defined monitoring problem, where **δx** is unknown and **δy** is known through measurements. If all assembly deviations were actually measured, the drifts on the design dimensions could be estimated by inverting the sensitivity matrix:

$$\boldsymbol{\delta x} = \mathbf{S}^{-1} \bullet \boldsymbol{\delta y} \tag{5}$$

However, the reconstruction of **δx** by (5) could be corrupted by random measurement errors included in **δy**. As a result, some δx_i may be artificially high and make it difficult to identify true drifts. This condition, called ill-posedness, occurs in many inverse problems and may require alternative methods of reconstruction.

In general, it can be assumed that the number of measured assembly deviations is $m \leq n$. If $m < n$, a given set of assembly deviations δy_j might have been caused by infinitely many sets of drifts δx_i. In order to deal with these cases, it will be assumed that only one of the drifts is actually non-zero (single damage). The goal will then be reformulated as a problem of damage detection and localization: from a set of measured δy_j, signal the existence of a drift (recognizing it from noise due to measurement error) and identify the design dimension responsible for it. Again, the inversion in (5) can provide a solution if vector **δy** includes some elements equal to zero (the unmeasured deviations). However, the risk of ill-posedness is even greater because the solution of the inverse problem is not unique.

4 Method

The proposed solution to the problem described in Section 3 includes the evaluation of the sensitivity matrix and its use to identify a possible damage from displacement measurements. Methods for these tasks are described below along with the procedure for their validation.

4.1 Tolerance analysis model

The calculation of matrix (4) requires a preliminary study of the structure, regardless of the number of sensors that will be used to measure the assembly deviations. The study is similar to a tolerance analysis, which is usually done to solve the direct problem (3). For such problem, the variables would have different meanings than in a monitoring context. The δx_i would be random deviations on design dimensions due to disturbances in the manufacturing processes of the parts; those deviations would normally be limited by tolerance specifications. The δy_j would be deviations on assembly dimensions due to the stackup of part deviations; once calculated, these would have to be compared to specifications on their maximum allowable variation (assembly tolerances).

In general, the sensitivity matrix can be evaluated using any available method of tolerance analysis. In direct linearization methods, the sensitivities are calculated directly from the geometric properties of the assembly rather than estimated by simulation plans on nonlinear stackup models. One of such methods, which will be used in this work, is based on the analogy with a problem of force analysis [49–51].

Figure 2 illustrates the static analogy for a plane truss. Let δl be the deviation on the length of a member and δp the consequent displacement of a node in a given direction (e.g. vertical). The sensitivity $S_{pl}=\delta p/\delta l$ is calculated by solving an equivalent static model, where the node is loaded with an external force F_p in the same direction as δp. Under this load, the member has an internal tensile or compressive force F_l. Once F_l is calculated, it turns out that

$$S_{pl} = F_l/F_p \tag{6}$$

The same member may be subject to a shift δh, i.e. a displacement of one of its ends from the nominal center of the node in the lengthwise direction. This further deviation can have different causes depending on the physical realization of the constraint. For a pin joint with hole diameter D and pin diameter d, the shift is the distance between the centers of the hole and the pin; its value varies randomly between zero (coaxial hole and pin) and $\delta h_{\max}=(D_{\mathrm{LMC}}-d_{\mathrm{LMC}})/2$, where D_{LMC} and d_{LMC} are the least material limits for the two features of the cylindrical fit. For other types of joints, δh may be due to clearance in fastener holes or other causes (e.g. plastic deformations). Based on the static analogy, the sensitivity $S_{ph}=\delta p/\delta h$ is calculated from the internal reaction F_h of the constraint, considered positive and equal in absolute value to the internal force F_l of the member:

$$S_{ph} = F_h/F_p = |F_l|/F_p \tag{7}$$

Finally, let δs be the displacement of a support in a given direction, e.g. due to a subsidence of ground or failure of an external frame. This deviation also causes an assembly deviation δp, whose sensitivity $S_{ps}=\delta p/\delta s$ corresponds to the opposite force to the reaction F_s of the support in the same direction:

$$S_{pl} = -F_s/F_p \tag{8}$$

Using the static analogy, the calculation of the sensitivity matrix (4) requires the resolution of n equivalent static models. The j-th static model provides all the sensitivities of the j-th assembly dimension, i.e. the displacement of a node in a horizontal or vertical direction. Correspondingly, the load on the truss is an external force F_p acting on that node in the same direction.

For the inverse problem addressed in this paper, using the sensitivity matrix would cause confusion between the deviations δl on member lengths and the shifts δh at the ends of the same members. The reason is that their sensitivities are equal in absolute value, as shown in (7) and (8); drifts on the two dimensions would therefore cause similar patterns of node displacements. In addition, their separate reconstruction would be more difficult due to the higher number of unknowns. Therefore, the δx_i will only be associated with member lengths and position coordinates of supports (two on the hinge and one on the roller). A drift identified on a member will be possibly due to either a change in length or a shift in an end joint. The actual cause of the drift will have to be ascertained in a subsequent inspection triggered by the diagnostic report.

4.2 Test for damage identification

The static analogy method recalled in subSection 4.1 gives the sensitivity matrix **S** defined in (3) and (4). Since the tolerance analysis is done on the whole structure, **S** is a square matrix with n rows corresponding to the assembly deviations δy_j and n columns corresponding to drifts (or design deviations) δx_i. If the structure is properly connected, **S** is expected to be invertible.

As assumed in Sect. 3, the condition of the structure is monitored on $m \le n$ assembly dimensions, defined by the m indices of measured deviations δy_j. The collected data form the column vector **δy**, which has m elements derived from measurements and the remaining $n-m$ elements equal to zero.

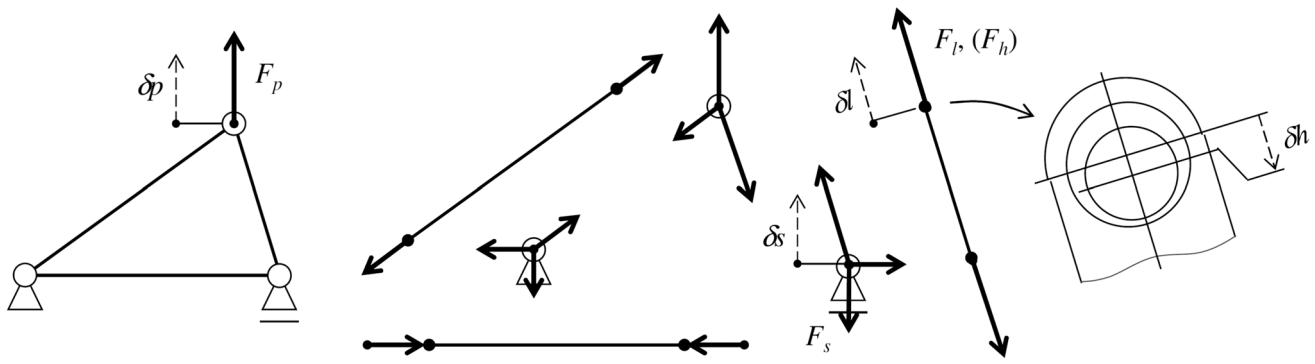

Fig. 2 Static analogy for plane trusses

Using (5) to estimate the column vector $\boldsymbol{\delta x}$ of the n design deviations, the columns of the inverse matrix $\mathbf{S}^{-1}$ corresponding to unmeasured assembly deviations would have no effect on the result. This can be expressed by classifying the n columns of $\mathbf{S}^{-1}$ as active (m) or passive ($n-m$), and by classifying the rows of $\mathbf{S}$ similarly. Equations (3) and (5) thus become

$$(\boldsymbol{\delta y})_{\boldsymbol{A}} = (\mathbf{S})_{\boldsymbol{A}} \bullet \delta \mathrm{x} \tag{9}$$

$$\boldsymbol{\delta x} = \left(\mathbf{S}^{-1}\right)_{\boldsymbol{A}} \bullet (\boldsymbol{\delta y})_{\boldsymbol{A}} \tag{10}$$

where:

- $(\boldsymbol{\delta y})_{\mathrm{A}}$ is the vector of the m measured assembly deviations;
- $(\mathbf{S})_{\mathrm{A}}$ is the $m \times n$ submatrix of $\mathbf{S}$ where its $n-m$ passive rows have been removed;
- $(\mathbf{S}^{-1})_{\mathrm{A}}$ is the $n \times m$ submatrix of $\mathbf{S}$ where its $n-m$ passive columns have been removed.

Figure 3 illustrates the new definitions. The loss of sensitivity information can alter the values of some δx_i even without measurement errors; at the very least, a δx_i could be zero if the corresponding row of $(\mathbf{S}^{-1})_{\mathrm{A}}$ had only zero elements. This suggests a validity criterion for the choice of the m sensors: each of the rows of $(\mathbf{S}^{-1})_{\mathrm{A}}$ must have at least one non-zero element. Such choices do not prevent strong alterations in the reconstruction, but at least avoid binding some of the δx_i to a constant value of zero.

The loss of information could be mitigated by replacing the scheme in Fig. 3 with a procedure similar to the static condensation of stiffness matrices in equilibrium equations,

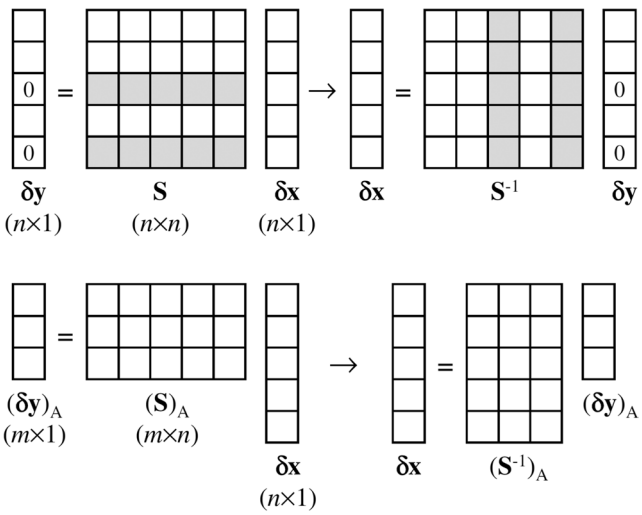

Fig. 3 Active deviation vector and submatrices

e.g. [101]. Its application to sensitivity matrices would require a partition of $\boldsymbol{\delta x}$ into two subvectors of dimensions m and $(n-m)$, to be calculated separately using in principle all the elements of $\mathbf{S}$. Appropriate criteria for selecting the partition should be found to ensure the validity conditions of condensation or to avoid further loss of information (e.g. some submatrices of $\mathbf{S}$ could be either non-invertible or with elements all equal to zero). The approach will be developed and tested in future studies.

Each time the node displacements are measured, the vector $(\boldsymbol{\delta y})_{\mathrm{A}}$ is processed in a test that can have two possible outcomes. A negative outcome (N) suggests that the structure has no drift on any design dimension, while a positive outcome (P) detects the occurrence of a drift and finds the design dimension responsible for it. The proposed test includes two steps for drift detection and localization, respectively.

A drift occurs when one of the design dimensions actually deviates from its initial value. This is generally not the same as the nominal value used for the calculation of sensitivities. During the erection of the structure, all design dimensions deviate from their nominal values, and cause initial deviations on assembly dimensions. The calibration of the measurement system on the structure detects with presumably high accuracy the initial (non-nominal) values of the assembly dimensions. These become the new nominals for the additional deviations δy_j measured during the monitoring phase.

Therefore, the deviations δy_j measured in the absence of drifts include only the measurement errors and not the effects of the initial deviations on design dimensions. Measurement errors will be assumed to be normally distributed with zero mean and standard deviation σ_0. If a drift occurs, some of the δy_j are likely to be out of the range of measurement errors. So the occurrence of a drift can be verified through the following test:

$$\mathrm{P} = \max\{\delta x_j\} > k\sigma_0 \tag{11}$$

and obviously N = ~P. The parameter k must be large enough to reduce the probability α of Type I error, i.e. of false positives that could trigger costly inspections. If (11) were a significance test on a single normally distributed variable, the choice $k=3$ would correspond to $\alpha=0.0027$. However (11) is a family of m tests: if the overall test has probability $\alpha_{\mathrm{F}}=0.0027$ of Type I error, every single test must have a corresponding probability of at least $\alpha=\alpha_{\mathrm{F}}/m$ (Bonferroni inequality). This corresponds to values of k increasing with m, up to about $k=4$ for $m=40$. On the other hand, values that are too high could increase the probability of false negatives, thus weakening the effectiveness of monitoring. From the results of preliminary trials using the simulation procedure that will be described in subSect. 4.3, the parameter has been set to $k=4$.

If the test is positive, the drift is located by associating each δx_i with a score $p_i \in [0, 1]$, which expresses the likelihood of a drift on the corresponding design dimension. Several criteria can be considered for the evaluation of the score. A baseline criterion estimates δx_i from (10) and calculates the score by normalizing their absolute values:

$$(p_i)_0 = |\delta x_i| \,/\, \sum_{i=1}^{n} |\delta x_i| \tag{12}$$

As already mentioned, the use of submatrix $(\mathbf{S}^{-1})_\mathrm{A}$ leads to a loss of information in the reconstruction of the δx_i from the δy_j. So the $(p_i)_0$ scores in (12) could deviate considerably from the proportions between the absolute values of the true δx_i. Furthermore, the reconstruction of $\boldsymbol{\delta}\mathbf{x}$ from $(\boldsymbol{\delta}\mathbf{y})_\mathrm{A}$ in (9) is an ill-posed problem as its solution is not unique (since $m<n$). As is known from the theory of inverse problems, e.g. [102], its direct solution by (10) is easily corrupted by random noise on $(\boldsymbol{\delta}\mathbf{y})_\mathrm{A}$. The stability of the solution can be improved by doing the reconstruction with the following expression:

$$(\boldsymbol{\delta}\mathbf{x})_1 = (\mathbf{R})_{\boldsymbol{A}} \bullet (\boldsymbol{\delta}\mathbf{y})_{\boldsymbol{A}} \tag{13}$$

where

$$(\mathbf{R})_{\boldsymbol{A}} = \left[(\boldsymbol{S})_{\boldsymbol{A}}^{\boldsymbol{T}} (\mathbf{S})_{\boldsymbol{A}} + k\sigma_0 I_n \right]^{-1} (\boldsymbol{S})_{\boldsymbol{A}}^{\boldsymbol{T}} \tag{14}$$

and I_n is the identity matrix of order n. The criterion expressed by (14) consists in the Tikhonov regularization of the transformation function $(\mathbf{S})_\mathrm{A}$ in the presence of a random error with an upper limit $k\sigma_0$. The score is then calculated again as

$$(p_i)_1 = |(\delta x_i)_1| \,/\, \sum_{i=1}^{n} |(\delta x_i)_1| \tag{15}$$

A further criterion derives from a property of the sensitivity matrix $\mathbf{S}$ in (3): its columns $\mathbf{s}_i$ are equal to the deviations $\boldsymbol{\delta}\mathbf{y}$ if $\delta x_i = 1$ and $\delta x_j = 0$ for $j \neq i$. Except for the aforementioned loss of information on sensitivities, the same property should hold in first approximation for the columns $(\mathbf{s}_i)_\mathrm{A}$ of $(\mathbf{S})_\mathrm{A}$ with respect to $(\boldsymbol{\delta}\mathbf{y})_\mathrm{A}$. The likelihood that the i-th design dimension has a drift >0 should be increasing with the cosine similarity c_i between $(\mathbf{s}_i)_\mathrm{A}$ and $(\boldsymbol{\delta}\mathbf{y})_\mathrm{A}$:

$$c_i = (\boldsymbol{\delta}\mathbf{y})_A^T \bullet \mathbf{s}_i \,/\, \left(|(\boldsymbol{\delta}\mathbf{y})_{\boldsymbol{A}}| \, |\mathbf{s}_i| \right) \tag{16}$$

where $|\mathbf{v}|$ denotes the norm of vector $\mathbf{v}$. The score is calculated by normalizing the absolute values of the cosine similarities between their minimum and maximum values:

$$(p_i)_2 = (|c_i| - min\,\{|c_i|\}) \,/\, (max\,\{|c_i|\} - min\,\{|c_i|\}) \tag{17}$$

When a drift occurs, the three scores are expected to show the same peak value for the same design dimension. This has been verified with preliminary simulation tests on some example trusses, under many possible combinations between the variables of the problem (choice of sensors, location and extent of the drift). In most cases, the peak is clearly recognizable and occurs on the same design dimension. In less favorable cases, where fewer sensors are used and the drift is comparable to the measurement error, the $(p_i)_1$ score calculated by regularization is more reliable than the $(p_i)_0$ score calculated by inversion, and provides consistent indications with the $(p_i)_2$ score calculated from cosine similarity. An example is shown in Fig. 4, where the dimension with bars of a different color is the one with the true drift. If the number of sensors becomes too small, the loss of sensitivity information can make peaks inconsistent between the three scores or absent altogether.

Based on the above observations, the drift is localized with a criterion that involves a combination of scores $(p_i)_1$ and $(p_i)_2$. The index i_D of the dimension subject to drift is calculated as follows:

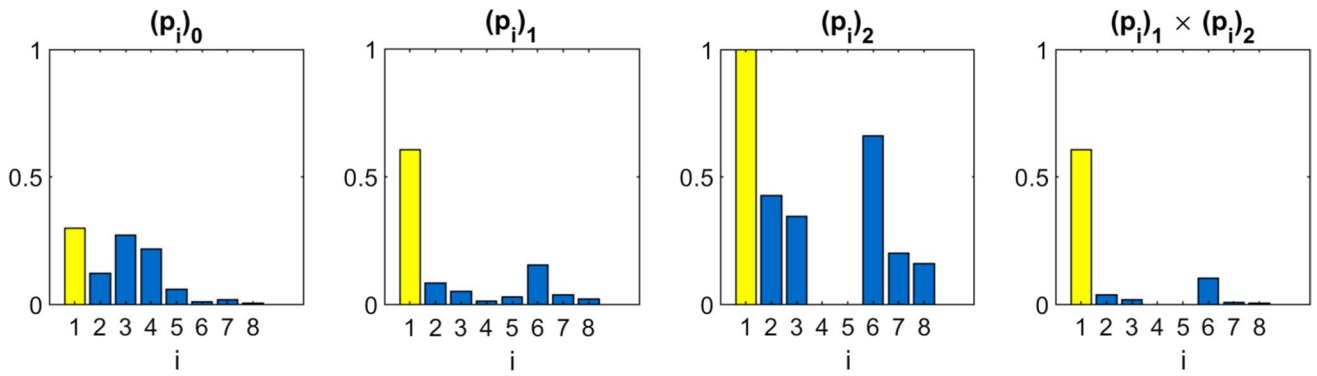

Fig. 4 Example of scores for damage localization

$$i_D = \operatorname{argmax}\left\{(p_i)_1\,(p_i)_2\right\} \tag{18}$$

4.3 Simulation of test performance

The method described in subSections 4.1 and 4.2 must allow the correct identification of dimensional drifts on the members of a truss. This must be verified against several possible shortcomings. First, the calculation procedure may be incorrect, i.e. the diagnostic test may not be effective (false positives, false negatives, wrong localization of the damage). Second, the calculation may not work for particular configurations of the structure in the intended scope of application (statically determinate plane trusses). Third, the method may place too high requirements for integration into an SHM system (calculation model difficult to build, excessive measurement accuracy).

To check the above conditions, the test for damage identification was simulated on geometric models of structures under many combinations of drifts and random measurement errors. The simulation concerns only the calculation method and does not consider further issues that could arise in its practical implementation; these include the instrumentation required (complexity, cost), the difficulty of setup (installation, calibration) and the reliability of the system (environmental effects on measurement uncertainty and durability). An experimental validation is postponed to future studies, assuming that a possible technical feasibility is consistent with the state of SHM technology as reported in literature (remote measurement of static displacements on structures).

For the purpose of simulation, the configuration of the structure is represented only by the sensitivity matrix (4). This would suggest to generate random matrices in an attempt to simulate the widest possible domain of configurations. However, that choice would not take into account specific properties of the matrix for actual structures, such as typical patterns in the values of sensitivities (many of which are supposed to be equal to zero or correlated). Therefore, sample configurations were selected for a preliminary verification of the method. The simulation was first carried out on very simple structures to develop the model in detail and fine-tune its parameters. Then the performance of the test was verified on more complex structures, chosen to represent possible application cases. For each case, the arrangement of the sensors was chosen randomly without considering any selection or optimization criteria.

As outlined in Fig. 5, the data for the simulation include:

- the configuration of the truss, represented by the number n of design dimensions (equal to the number of assembly dimensions) and the sensitivity matrix $\mathbf{S}$ calculated by static analogy;

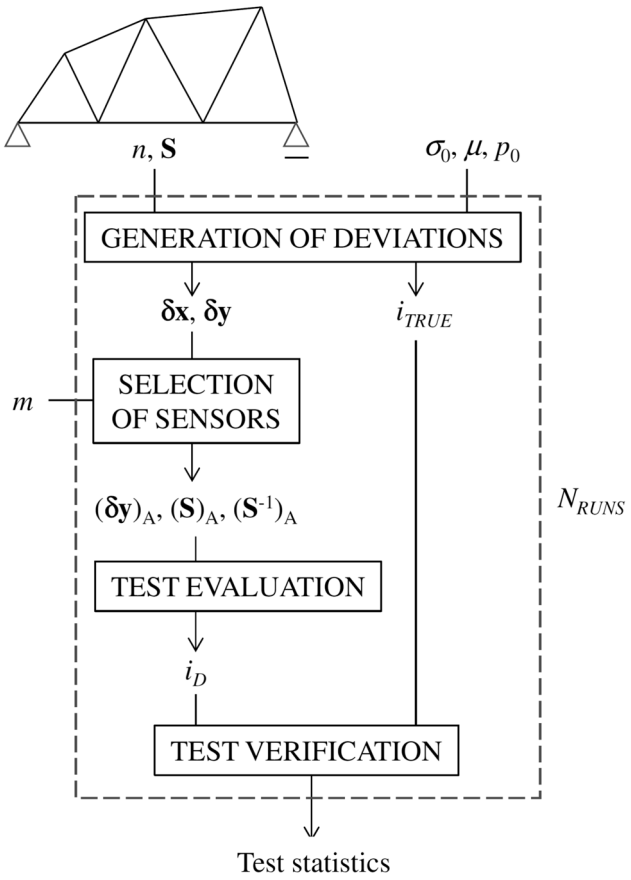

Fig. 5 Flow chart of the simulation model

- the standard deviation σ_0 of the random error in the measurement of the assembly deviations;
- the magnitude μ of the drift to be assigned to a random member i_{TRUE} of the truss;
- the probability p_0 that the structure has no drift on any of the members ($i_{\mathrm{TRUE}}=0$);
- the number m of sensors for measuring assembly deviations, to be chosen from the possible valid sets.

The test is repeated for N_{RUNS} random instances of the simulation model. Each simulation run includes the following steps:

- The vector $\boldsymbol{\delta}\mathbf{x}$ of design deviations is either set to zero indicating no drift ($i_{\mathrm{TRUE}}=0$) or modified with probability ($1-p_0$) by assigning a drift μ to a random design dimension (i_{TRUE}). The vector $\boldsymbol{\delta}\mathbf{y}$ of assembly deviations is calculated from (3) and then perturbed with a random measurement error from N(0, σ_0).
- A subset of m assembly deviations is randomly selected from the valid sets, thus evaluating the active deviation vector $(\boldsymbol{\delta}\mathbf{y})_{\mathrm{A}}$ and the active submatrices $(\mathbf{S})_{\mathrm{A}}$ and $(\mathbf{S}^{-1})_{\mathrm{A}}$.

- The test described in subSection 4.2 is run on the selected assembly deviations. The occurrence (P) or non-occurrence (N) of the drift is detected by (11). The index i_D of the design dimension with the drift is set to zero if the test is negative, or calculated from (18) using the scores from (15) and (17).
- The outcome of the test (i_D) is compared to the truth (i_{TRUE}), classifying the test as:
  - o true positive: $TP = P \cap (i_D = i_{TRUE} \neq 0)$;
  - o true negative: $TN = N \cap (i_{TRUE} = 0)$;
  - o false positive: $FP = P \cap [(i_{TRUE} = 0) \cup (i_D \neq i_{TRUE})]$
  - o false negative: $FN = N \cap (i_{TRUE} \neq 0)$.

The total numbers of TP, TN, FP, and FN instances are counted. The effectiveness of the test is then estimated through the following statistics, which are generally used for classification tests in data analysis (e.g. [103]):

$$\mathrm{TPR} = \frac{\mathrm{TP}}{\mathrm{TP} + \mathrm{FN}}, \mathrm{FPR} = \frac{\mathrm{FP}}{\mathrm{FP} + \mathrm{TN}} \tag{19}$$

where the true positive rate TPR is the fraction of actually positive cases that are correctly classified as positive, and the false positive rate FPR is the fraction of actually negative cases that are incorrectly classified as positive. If the test always gave the right result, the statistics would have the ideal values TPR = 1 and FPR = 0. An alternative choice of equivalent statistics is

$$\mathrm{precision} = \frac{\mathrm{TP}}{\mathrm{TP} + \mathrm{FP}}, \mathrm{recall} = \frac{\mathrm{TP}}{\mathrm{TP} + \mathrm{FN}} \tag{20}$$

where the cases correctly classified as positive are compared with all the cases classified as positive and with all the actually positive cases, respectively. These statistics express the accuracy of the test (ability to avoid false positives) and its completeness (ability to avoid false negatives), respectively, both with ideal values equal to 1. Since usually every change in the parameters of the test has a divergent effect on the two tests of each pair (one improves, the other worsens compared to the ideal value), the overall effectiveness of the test is evaluated by means of the F_1 score often proposed as a compromise (ideal value 1):

$$\mathrm{F_1} = \frac{2 \bullet \mathrm{precision} \bullet \mathrm{recall}}{\mathrm{precision} + \mathrm{recall}} = \frac{2\ \mathrm{TP}}{2\ \mathrm{TP} + \mathrm{FP} + \mathrm{FN}} \tag{21}$$

It is reasonable to expect that the statistic in (21) depends on the input data of the simulation model. The test will be more effective if the drift to be detected is much larger than the measurement error, given the accuracy of the sensors and the drift regarded as worth of attention. In addition, the test will obviously be more reliable if a higher number of assembly deviations is measured on the structure. Finally, the test may have difficulty treating situations where the occurrence of a drift is an extremely rare event, because the need to detect the few positive cases with certainty could have the risk of false positives as a side effect. As will be detailed in Section 5, the above effects were evaluated by performing factorial plans of simulations with appropriate levels for the related variables μ/σ_0, m, and p_0.

5 Results

The proposed method is demonstrated on two cases. The first is an extremely simple structure, on which the calculations can be shown in full detail. The second is a more realistic structure, with the aim of verifying whether the feasibility of the workflow and the effectiveness of the method remain valid as the size of the problem increases.

5.1 Simple truss

Figure 6 shows a truss with $n_N = 4$ and $n_M = 5$. The drawing shows the angles and lengths of the members for an overall size of 6 × 3 m. Due to the structural determinacy, however, scaling the dimensions would not affect the following calculations. Equally irrelevant are the materials, the structural sections of the members, and the detailed design of the joints.

The vector of design deviations has $n = 8$ elements, which include the deviations δl_i on the lengths of the members, the displacements $\delta s_{u\mathrm{A}}$ (horizontal) and $\delta s_{v\mathrm{A}}$ (vertical) of support A, and the vertical displacement $\delta s_{v\mathrm{B}}$ of support B:

$$\boldsymbol{\delta}\mathrm{x} = [\ \delta l_1 \quad \delta l_2 \quad \delta l_3 \quad \delta l_4 \quad \delta l_5 \quad \delta s_{u\mathrm{A}} \quad \delta s_{v\mathrm{A}} \quad \delta s_{v\mathrm{B}}\ ]^T \tag{22}$$

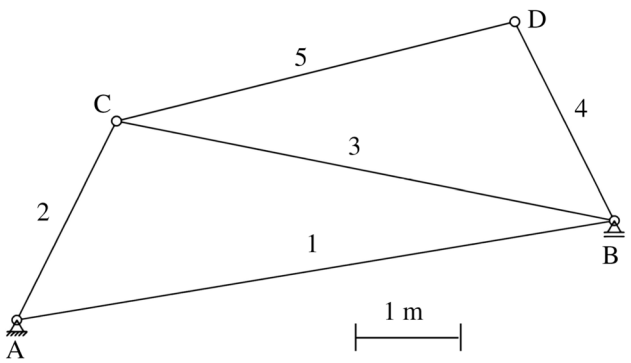

Fig. 6 Simple truss

The vector of assembly deviations includes the horizontal and vertical displacements (*u*-*v* directions) of nodes A, B, C, and D:

$$\boldsymbol{\delta}\mathrm{y} = [\ \delta u_{\mathrm{A}}\quad \delta v_{\mathrm{A}}\quad \delta u_{\mathrm{B}}\quad \delta v_{\mathrm{B}}\quad \delta u_{\mathrm{C}}\quad \delta v_{\mathrm{C}}\quad \delta u_{\mathrm{D}}\quad \delta v_{\mathrm{D}}\ ]^{T} \tag{23}$$

The sensitivity matrix in (4) is calculated using the static analogy described in subSection 4.1. Each row of **S** includes the sensitivities of the corresponding element of **δy** (the displacement of a node in a given direction) with respect to all the elements of **δx** (length variations or support displacements). These come from the solution of an equivalent static model, where the node is loaded with a unit force in the same direction. Since (6), the sensitivities with respect to changes in length (resulting from axial deformations or shifts at end joints) are equal to the internal forces at the members. From (8), the sensitivities with respect to the displacements of supports are opposed to the corresponding components of the support reactions. Figure 7 shows the equivalent static models for the calculation of the sensitivities of δu_{C} (row 5) and δv_{C} (row 6), where the external forces are set to 1 kN. The models are solved by an available 2D frame analysis tool (Ftool).

The *n* static models provide the following sensitivity matrix:

$$\mathrm{S} = \begin{bmatrix} 0 & 0 & 0 & 0 & 0 & 1 & 0 & 0 \\ 0 & 0 & 0 & 0 & 0 & 0 & 1 & 0 \\ 1.014 & 0 & 0 & 0 & 0 & 1 & 0.167 & -0.167 \\ 0 & 0 & 0 & 0 & 0 & 0 & 0 & 1 \\ 0.922 & 0.203 & -0.927 & 0 & 0 & 1 & 0.333 & -0.333 \\ -0.461 & 1.016 & 0.464 & 0 & 0 & 0 & 0.833 & 0.167 \\ 0.829 & 0.407 & -0.721 & -0.248 & 0.916 & 1 & 0.5 & -0.5 \\ -0.092 & 0.203 & -0.361 & 0.458 & 0.994 & 0 & 0.167 & -0.833 \end{bmatrix} \tag{24}$$

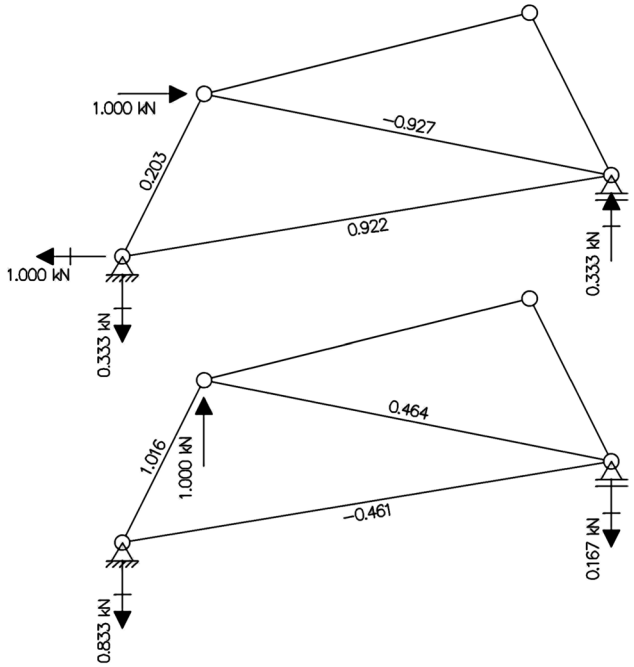

Fig. 7 Two equivalent static models for the simple truss

The inverse of the matrix in (24) is

$$\mathrm{S}^{-1} = \begin{bmatrix} -0.986 & -0.165 & 0.986 & 0.165 & 0 & 0 & 0 & 0 \\ -0.447 & -0.894 & 0 & 0 & 0.448 & 0.895 & 0 & 0 \\ 0 & 0 & 0.981 & -0.195 & -0.981 & 0.196 & 0 & 0 \\ 0.001 & -0.001 & 0.776 & 0.737 & 0.715 & 0.180 & -1.492 & 1.375 \\ 0 & 0 & 0.090 & 0.443 & -0.777 & -0.195 & 0.688 & 0.372 \\ 1 & 0 & 0 & 0 & 0 & 0 & 0 & 0 \\ 0 & 1 & 0 & 0 & 0 & 0 & 0 & 0 \\ 0 & 0 & 0 & 1 & 0 & 0 & 0 & 0 \end{bmatrix} \tag{25}$$

If the number *m* of sensors (i.e., measured assembly deviations) is equal to *n*, (25) can be used to solve the inverse problem (5) for estimating the unknown design deviations. If $m < n$, the measurements are reduced to a subset of the assembly deviations, which is represented by the active submatrices $(\mathbf{S})_{\mathrm{A}}$ and $(\mathbf{S}^{-1})_{\mathrm{A}}$ in (9) and (10). As mentioned in the comment to Fig. 3, the valid subsets of sensors correspond only to the submatrices $(\mathbf{S}^{-1})_{\mathrm{A}}$ with rows containing at least one non-zero element. Table 1 lists the valid choices for the possible values of *m*, providing the indices of the selected elements of the vector **δy** in (23).

Table 1 Sensor choices for the simple truss

m	Indices	$\lvert(\mathbf{S}^{-1})_{\mathrm{A}}\rvert$	$\lvert(\mathbf{R})_{\mathrm{A}}\rvert$	C_a
8	1 2 3 4 5 6 7 8	2.51	0.91	0.34
7	1 2 3 4 5 6 7	2.23	0.91	0.43
	1 2 3 4 5 6 8	2.13	0.91	0.29
	1 2 3 4 5 7 8	2.49	0.91	0.46
	1 2 3 4 6 7 8	2.42	0.91	0.32
	1 2 4 5 6 7 8	2.40	0.91	0.35
6	1 2 3 4 5 6	1.96	0.91	0.63
	1 2 3 4 5 7	2.19	0.91	0.59
	1 2 3 4 5 8	2.10	0.91	0.41
	1 2 3 4 6 7	2.13	0.91	0.44
	1 2 3 4 6 8	2.11	0.91	0.30
	1 2 3 4 7 8	2.40	0.90	0.45
	1 2 4 5 6 7	2.14	0.91	0.45
	1 2 4 5 6 8	1.95	0.91	0.30
	1 2 4 5 7 8	2.38	0.90	0.49
	1 2 4 6 7 8	2.21	0.91	0.35
5	1 2 3 4 5	1.91	0.91	0.71
	1 2 3 4 6	1.95	0.91	0.63
	1 2 3 4 7	2.10	0.91	0.60
	1 2 3 4 8	2.09	0.91	0.39
	1 2 4 5 6	1.83	0.91	0.64
	1 2 4 5 7	2.11	0.90	0.63
	1 2 4 5 8	1.91	0.88	0.43
	1 2 4 6 7	1.82	0.90	0.47
	1 2 4 6 8	1.78	0.88	0.32
	1 2 4 7 8	2.20	0.91	0.50
4	1 2 3 4	1.91	0.91	0.83
	1 2 4 5	1.72	0.88	0.73
	1 2 4 6	1.71	0.87	0.66
	1 2 4 7	1.78	0.88	0.67
	1 2 4 8	1.77	0.88	0.50
3	1 2 4	1.62	0.77	0.89

Reconstructing the design deviations with (10), random errors on the elements of $(\boldsymbol{\delta y})_A$ cause generally larger errors on the elements of $\boldsymbol{\delta x}$. From a known property of inverse problems [102], the ratio between the absolute values of the two errors is estimated by the norm of the inverse submatrix $(\mathbf{S}^{-1})_A$, which is equal to the reciprocal of its first singular value. The norms $|(\mathbf{S}^{-1})_A|$ of the submatrices corresponding to the valid sensor choices are shown in Tab. 1. It can be noted that measurement errors can lead to reconstruction errors that are more than doubled, especially with sensor choices that would result in a less severe loss of information (m equal to or slightly less than n). As mentioned in subSection 4.2, this drawback is mitigated by performing the reconstruction with (13). Table 1 shows that the norms $|(\mathbf{R})_A|$ of the matrices defined in (14) have values below 1, which seem to confirm the effectiveness of regularization in reducing the impact of measurement errors.

The use of cosine similarity in (16) for the localization of the drift is all the more effective the closer the columns of submatrix $(\mathbf{S})_A$ are to orthogonality. If the number of sensors decreases, the vectors corresponding to the columns of $(\mathbf{S})_A$ lose dimensionality and tend to reduce the mutual differences. It can be expected that this will progressively reduce the effectiveness of cosine similarity as m decreases. Table 1 confirms this conjecture through the parameter C_a, defined as the average absolute value of the cosine similarities between pairs of columns of $(\mathbf{S})_A$. The case $C_a=0$ would correspond to orthogonal vectors, while $C_a=1$ would indicate that the vectors are coincident or at least one of the two vectors vanishes. For the structure considered, the parameter actually increases as m decreases, suggesting that cosine similarity may lose effectiveness ($C_a>0.5$–0.6) with a number of sensors around 4–5 (about half of the maximum number n).

The accuracy of the damage identification method was verified with a full factorial plan of simulations using the model described in subSection 4.3. Table 2 shows the levels used for the three factors of the plan. Specifically:

- the two levels for the probability of no drift correspond respectively to an alarm situation triggered by a previous measurement or by other sources ($p_0=0.5$) and to a planned measurement performed for monitoring purposes ($p_0=0.99$);
- the two levels for the signal-to-noise ratio correspond to a minor drift barely distinguishable from measurement noise ($\mu/\sigma_0=5$) and to a more serious damage ($\mu/\sigma_0=10$);
- the number m of sensors has six levels that span the entire valid range.

Table 2 Simulation plan for the simple truss

Factor	*Levels*
p_0	0.5, 0.99
μ/σ_0	5, 10
m	8, 7, 6, 5, 4, 3

For each of the $2\times2\times6=24$ combinations between the factor levels, 3 replications of the simulation were performed with $N_{RUNS}=100{,}000$, comparing the values obtained for the F_1 score. The variation in results was negligible both between the replicates and between the two levels of p_0 (coefficients of variation less than 1%). Figure 8 shows the variation of F_1 with respect to the two significant factors in the simulations with $p_0=0.99$. The effect of the signal-to-noise ratio μ/σ_0 shows a difference of about 10% of F_1 between the two levels. The performance of the test clearly decreases with the number m of sensors. For $m=8$, F_1 values are around 0.9: drifts are correctly localized in about 90% of cases (TPR), and are wrongly reported in about 0.1% of negative cases (FPR). The performance still seems acceptable up to $m=5$ (F_1 in the range 0.7–0.8); below this limit, the fraction of undetected or (more often) incorrectly localized drifts exceeds 30%, while false positives remain at a negligible level.

5.2 More complex truss

Figure 9 shows a truss with with $n_N=10$, $n_M=17$, and an overall size of 12×6 m. As in the previous case, the nodes are assumed to be pin-jointed and the supports include a hinge and a horizontal roller. The problem consists in the identification of a drift on one of the design dimensions

$$\boldsymbol{\delta}\mathrm{x} = [\ \delta l_1 \quad \delta l_2 \quad \cdots \quad \cdots \quad \delta l_{17} \quad \delta s_{u\mathrm{A}} \quad \delta s_{v\mathrm{A}} \quad \delta s_{v\mathrm{B}}\ ]^T \tag{26}$$

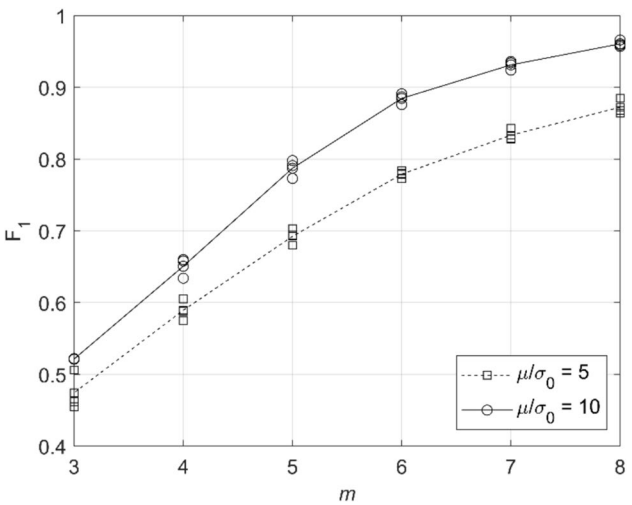

Fig. 8 Test performance for the simple truss ($p_0=0.99$)

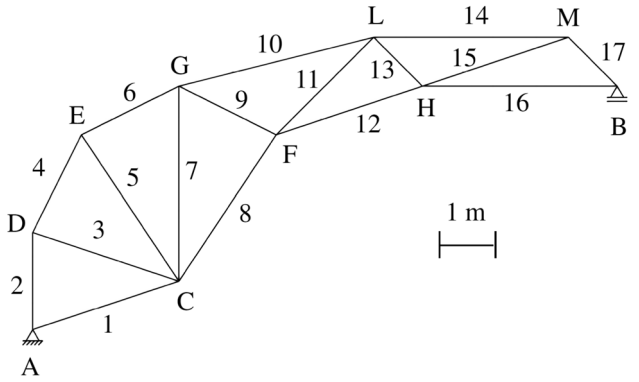

Fig. 9 Complex truss

from displacement measurements of the nodes A, B, … M:

$$\boldsymbol{\delta}\mathrm{y} = [\ \delta u_\mathrm{A}\quad \delta v_\mathrm{A}\quad \delta u_\mathrm{B}\quad \delta v_\mathrm{B}\quad \cdots\quad \cdots\quad \delta u_\mathrm{M}\quad \delta v_\mathrm{M}\ ]^T \tag{27}$$

Both vectors have $n=20$ elements. Table 3 shows the sensitivity matrix **S**, again calculated using the static analogy method. Each row of **S** includes the internal forces at the members and the forces opposed to the support reactions under a horizontal or vertical unit force applied to one of the nodes.

The matrix is less sparse than in the previous case and is invertible. The inverse matrix has norm $|\mathbf{S}^{-1}|=2.44$, while its regularized version has a norm $|\mathbf{R}|=0.91$. Comparing these properties with those of the previous case (row of Tab. 1 with $m=8$), it seems that the observations made for the simple truss remain valid even for structures of realistic complexity: measurement errors cause reconstruction errors more than doubled, and regularization allows to mitigate the problem well enough.

For combinatorial reasons, the choice of sensor subsets is much wider than for the simple truss. By applying the selection rule with a lower bound of 0.01 for the maximum element of each row of $(\mathbf{S}^{-1})_\mathrm{A}$, the number m of sensors can go down to 7. For each m, sensors can be selected from a large number of valid subsets, up to a maximum of about 12 thousands per $m=13$. Along the range of m, the mean cosine similarity of $(\mathbf{S})_\mathrm{A}$ is always in the range $C_a=0.4$–0.5; this seems to confirm the validity of cosine similarity as a criterion for the localization of drifts.

Table 4 shows the settings of the simulation plan. The probability of no drift has been set to a constant value $p_0=0.99$, considering the non-significance of the factor in the previous case. All valid numbers m of sensors between 20 and 7 were tested for the same two levels of the signal-to-noise ratio μ/σ_0. The full factorial plan includes $2\times14=28$ combinations between factor levels, each replicated 3 times with $N_\mathrm{RUNS}=100{,}000$.

The graph in Fig. 10 shows the F_1 scores obtained for the different combinations between factor levels. When the drift is clearly distinguishable from background noise ($\mu/\sigma_0=10$), the effectiveness of the test is equivalent to that observed for the simple structure for $m=n$ ($F_1\approx0.95$), and remains very high ($F_1>0.9$) until about $m=15$. With half the number of sensors ($m=10$), the complex truss gives $F_1\approx0.8$, which is much better than for the simple truss ($F_1\approx0.65$ for $m=4$ in Fig. 8). Up to that level, the test keeps an acceptable performance ($F_1>0.7$) even with minor drifts ($\mu/\sigma_0=5$). A deeper analysis confirms the test's excellent ability to avoid false negatives, while most false positives correspond to wrongly localized true positives.

The results in Fig. 10, like those in Fig. 8 for the simple truss, assume a completely random choice of the subset of m sensors. Alternatively, the subset could be chosen according to some criteria in order to improve the effectiveness of the test. Although the optimization of the choice has not been dealt with in the present work, simulation has been used to evaluate its possible effect. Figure 11 shows three different graphs of the average F_1 score in the valid range of m (from 20 to 7) with given levels of the other two factors ($p_0=0.9$, $\mu/\sigma_0=10$), $N_\mathrm{RUNS}=1{,}000{,}000$, and 3 replications for each m. One of the graphs (denoted with 100%) is constructed by running the simulation in a similar way to the one described above, with the exception of limiting the choice to just 20 random subsets. The other two graphs are constructed by selecting the best 50% and the best 25% of those subsets, respectively, and repeating the calculation of F_1 through (19), (20) and (21). The results obviously coincide for $m=n=20$ because that case involves only one possible set of sensors. For $m<n$, it can be seen that the selection of sensors improves the effectiveness of the test. Up to about 15 sensors, the effectiveness of the test remains very close to the maximum (0.995). By further reducing m, the selection may slightly reduce the number of sensors needed. For example, a target performance $F_1\geq0.9$ could be satisfied by 11 or 10 sensors respectively (choosing the best half or fourth respectively) rather than by 13 sensors with completely random choice. The improvement is likely to be higher with a more sophisticated selection strategy.

6 Conclusions

In the monitoring of structures, damage identification methods are needed to detect and localize abnormal conditions from vibration or displacement measurements. Model-based methods use FEM simulation to predict the effects of predefined damage modes. The measurements are then automatically compared with those effects by calculating damage indicators related to the likelihood of individual

Table 3 Sensitivity matrix for the complex truss

	1	*2*	*3*	*4*	*5*	*6*	*7*	*8*	*9*	*10*	*11*	*12*	*13*	*14*	*15*	*16*	*17*	*18*	*19*	*20*
1	0	0	0	0	0	0	0	0	0	0	0	0	0	0	0	0	0	1	0	0
2	0	0	0	0	0	0	0	0	0	0	0	0	0	0	0	0	0	0	1	0
3	1.054	0.083	-0.037	0.060	-0.049	0.070	-1.019	1.689	1.498	-1.316	-0.048	2.436	0.499	-1.664	1.315	1.417	-0.589	1	0.147	-0.147
4	0	0	0	0	0	0	0	0	0	0	0	0	0	0	0	0	0	0	0	1
5	1.054	-0.025	0.113	-0.240	0.145	-0.210	-0.104	0.338	0.325	-0.401	0.108	0.329	0.029	-0.333	0.263	0.084	-0.118	1	0.083	-0.083
6	0	0.750	-0.339	0.719	-0.434	0.629	0.312	-1.014	-0.675	1.202	-0.324	-0.988	-0.088	0.998	-0.788	-0.251	0.354	0	0.750	0.250
7	1.054	-0.167	-0.827	-0.479	0.289	-0.419	-0.208	0.676	0.450	-0.801	0.216	0.659	0.058	-0.666	0.526	0.167	-0.236	1	0.167	-0.167
8	0	1	0	0	0	0	0	0	0	0	0	0	0	0	0	0	0	0	1	0
9	1.054	0	0	0	-0.451	-0.839	-0.416	1.362	0.900	-1.602	0.432	1.317	0.117	-1.331	1.051	0.334	-0.472	1	0.333	-0.333
10	0	0.917	-0.414	0.878	0.370	0.210	0.104	-0.338	-0.225	0.401	-0.108	-0.329	-0.029	0.333	-0.263	-0.084	0.118	0	0.917	0.083
11	1.054	0	0	0	0	0	-1.165	1.802	1.738	-1.602	0.431	1.317	0.117	-1.331	1.051	0.334	-0.472	1	0.333	-0.333
12	0	0.583	-0.264	0.559	-0.337	0.489	1.019	-0.788	-1.684	2.003	-0.540	-1.646	-0.146	1.664	-1.314	-0.418	0.590	0	0.583	0.417
13	1.054	0.083	-0.037	0.080	-0.049	0.070	-1.019	1.689	1.125	-2.003	0.540	1.646	0.146	-1.664	1.314	0.418	-0.590	1	0.417	-0.417
14	0	0.750	-0.339	0.719	-0.434	0.629	1.311	-1.013	-0.675	1.202	0.324	-0.988	-0.088	0.998	-0.788	-0.251	0.354	0	0.750	0.250
15	1.054	0.083	-0.037	0.080	-0.049	0.070	-1.019	1.689	1.498	-1.316	-0.048	2.436	0.498	-1.664	1.314	0.418	-0.590	1	0.417	-0.417
16	0	0.333	-0.151	0.319	-0.193	0.280	0.583	-0.450	-0.962	1.145	0.902	-1.843	-1.294	2.662	-2.102	-0.668	0.944	0	0.333	0.667
17	1.054	0.167	-0.075	0.160	-0.097	0.140	-0.874	1.577	1.256	-1.030	0.177	1.975	0.175	-1.997	1.578	0.501	-0.708	1	0.500	-0.500
18	0	0.417	-0.188	0.399	-0.241	0.349	0.728	-0.563	-1.203	1.431	1.127	-2.304	-0.204	2.329	-1.839	-0.585	0.826	0	0.417	0.583
19	1.054	0.167	-0.075	0.160	-0.097	0.140	-0.874	1.577	1.256	-1.030	0.177	1.975	0.175	-0.997	1.578	0.501	-0.708	1	0.500	-0.500
20	0	0.083	-0.037	0.080	-0.049	0.070	0.146	-0.113	-0.241	0.286	0.226	-0.461	-0.324	0.666	0.263	-0.916	1.296	0	0.083	0.917

Table 4 Simulation plan for the complex truss

Factor	*Levels*
p_0	0.99
μ/σ_0	5, 10
m	20, 19, 18, …, 7

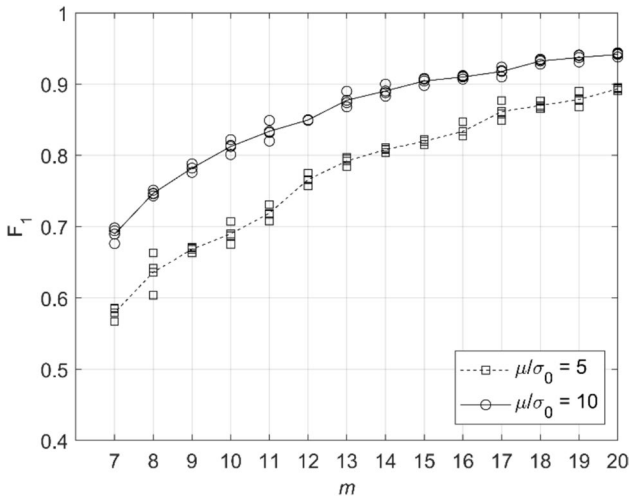

Fig. 10 Test performance for the complex truss ($p_0 = 0.99$)

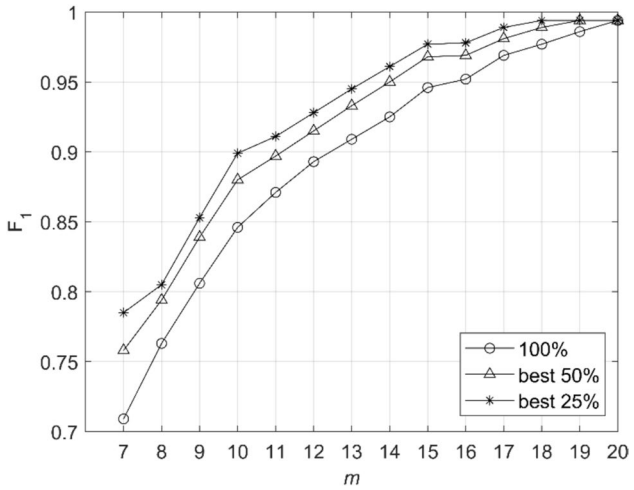

Fig. 11 Effect of sensor selection on test performance ($p_0 = 0.9$, $\mu/\sigma_0 = 10$)

modes. Compared to data-driven methods, which perform statistical tests on sequences of measurements, this generally reduces the amount of data required but requires additional efforts for model setup and simulation.

With the aim of simplifying these tasks, the work proposes to build the damage identification model through tolerance analysis of the structure. This allows the use of the available models, which can be interactively built with the help of variation simulation software. The concept has been tested on the case of statically determined trusses, where the analysis of structures with realistic complexity can be done through simple procedural scripts. Tolerance analysis calculates all measured displacements (assembly deviations) as linear functions of the expected drifts on member lengths or support positions. The resulting model (sensitivity matrix) allows an easy calculation of damage indicators through simple operations of regularization and matrix inversion, widely studied in the theory of inverse problems.

As a first step, the feasibility check of the integration between damage identification and tolerance analysis has required the choice of an appropriate tolerance analysis model. Although in principle many different models may yield the same sensitivity matrix, static analogy seems particularly suitable for the proposed application due the following reasons:

- the static analogy is a direct linearization model that provides sensitivities without the need for repeated evaluations or Monte Carlo simulation;
- the calculation of sensitivities by force analysis makes the workflow similar to other structural design tasks, and can be done both with common manual procedures and by FEM;
- in principle, the same method could be extended to three-dimensional and statically indeterminate structures, thus broadening the spectrum of possible applications.

After demonstrating the static analogy workflow, highlighting its relative simplicity on some examples, the paper has tested the effectiveness of the damage identification test. For this purpose, the procedure was simulated in the assumption that only a subset of the possible measurements is actually collected, and that they are affected by random errors. The simulation showed that the method allows to almost completely avoid undetected drifts and reduce the probability of false alarms to acceptable levels under a wide range of conditions. A broader validation will come from running the simulation on randomly generated structures, with the aim to evaluate alternatives both for the test and for the validity criterion of sensor subsets.

Overall, the results of the paper do not imply a direct comparison with other methods of damage identification regarding effectiveness and ease of integration into real monitoring systems. The contribution of the work is mainly in the proposal of a different approach to solving the problem. Practical situations where it can effectively complement or replace alternative methods remain to be identified by future application to monitoring projects. A possible argument in favor is that tolerance analysis is consistent with the increasing trend towards the use of static displacement sensors.

Unlike some damage identification methods available for SHM, the proposed test is not able to distinguish actual structural damage from environmental variations (e.g. thermal expansion). Although the latter are likely to be smaller than the former, the damage detection condition should involve some kind of normalization of assembly deviations. This will be the subject of future research, as well as the feasibility of actual integration with existing measurement systems, the optimal sensor placement, and the verification of the effects of uncertainty on the geometric parameters of the tolerance analysis model.

The method will also need to be improved in order to widen its application scope. If a continuous stream of measured data were available, more complex tests proposed in the context of process monitoring could further enhance damage classification. In addition to the already mentioned cases of 3D and statically indeterminate structures, the treatment of mechanisms could be interesting in relation to specific applications or alternative methods of measuring assembly deviations.

Authors' contributions Not applicable.

Funding Open access funding provided by Politecnico di Milano within the CRUI-CARE Agreement. The author received no specific funding for this work.

Data availability The author confirms that the data supporting the findings of this study are available within the paper.

Code availability Not applicable.

Declarations

Conflicts of interest The author declares that he has no conflicts of interest.

References

1. Shen Z, Ameta G, Shah JJ, Davidson JK (2005) A comparative study of tolerance analysis methods. ASME J Comput Inf Sci Eng 5:247–256
2. Singh PK, Jain PK, Jain SC (2009) Important issues in tolerance design of mechanical assemblies. Part I: tolerance analysis. Proc IMechE B J Eng Manuf 223:1225–1247
3. Chen H, Jin S, Li Z, Lai X (2014) A comprehensive study of three dimensional tolerance analysis methods. Comput Aided Des 53:1–13
4. Drake PJ (ed) (1999) Dimensioning and tolerancing handbook. McGraw-Hill, New York
5. Fischer BR (2004) Mechanical tolerance stackup and analysis. Marcel Dekker, New York
6. Schleich B, Wartzack S (2016) A quantitative comparison of tolerance analysis approaches for rigid mechanical assemblies. Procedia CIRP 43:172–177
7. Cao Y, Liu T, Yang J (2018) A comprehensive review of tolerance analysis models. Int J Adv Manuf Technol 97:3055–3085
8. Clément A, Rivière A, Temmerman M (1994) Cotation tridimensionelle des systèmes mécaniques. Pyc Livres, Paris
9. Whitney DE (2004) Mechanical assemblies. Oxford University Press, New York
10. ASME Y14.5.1M (2018) Mathematical definition of dimensioning and tolerancing principles, ASME International, New York
11. Boyer M, Stewart NF (1991) Modeling spaces for toleranced objects. Int J Robot Res 10(5):570–582
12. Whitney DE, Gilbert OL, Jastrzebski M (1994) Representation of geometric variations using matrix transforms for statistical tolerance analysis in assemblies. Res Eng Des 6:191–210
13. Wu Y, Chen C (2018) An automatic generation method of the coordinate system for automatic assembly tolerance analysis. Int J Adv Manuf Technol 95:889–903
14. Salomons OW, Haalboom FJ, Poerink HJJ, Slooten FV, van Houten FJAM, Kals HJJ (1996) A computer aided tolerancing tool II: tolerance analysis. Comput Ind 31(2):175–186
15. Desrochers A, Rivière A (1997) A matrix approach to the representation of tolerance zones and clearances. Int J Adv Manuf Technol 13(9):630–636
16. Chase KW, Gao J, Magleby SP (1995) General 2-D tolerance analysis of mechanical assemblies with small kinematic adjustments. J Des Manuf 5:263–274
17. Gao J, Chase KW, Magleby SP (1998) Generalized 3-D tolerance analysis of mechanical assemblies with small kinematic adjustments. IIE Trans 30(4):367–377
18. Yu J, Zhao Y, Wang H, Lai X (2018) Tolerance analysis of mechanical assemblies based on the product of exponentials formula. Proc IMechE Part B: J Eng Manuf 232(14):2616–2626
19. Bourdet P, Mathieu L, Lartigue C, Ballu A (1996) The concept of the small displacement torsor in metrology. Ser Adv Math Appl Sci 40:110–122
20. Li H, Zhu H, Li P, He F (2014) Tolerance analysis of mechanical assemblies based on small displacement torsor and deviation propagation theories. Int J Adv Manuf Technol 72:89–99
21. Rivest L, Fortin C, Morel C (1994) Tolerancing a solid model with a kinematic formulation. Comput Aided Des 26:465–476
22. Laperrière L, Ghie W, Desrochers A (2002) Statistical and deterministic tolerance analysis and synthesis using a unified Jacobian-torsor model. CIRP Ann Manuf Technol 51(1):417–420
23. Chen H, Li X, Jin S (2021) A statistical method of distinguishing and quantifying tolerances in assemblies. Comput Ind Eng 156:107259
24. Peng H, Chang S (2022) Including material conditions effects in statistical geometrical tolerance analysis of mechanical assemblies. Int J Adv Manuf Technol 119:6665–6678
25. Liu S, Yu H, Xia Z, Chen K (2024) A new virtual functional element method for deviation prediction of assembled structures with parallel connection chain. CIRP J Manuf Sci Technol 48:42–54

26. Liu S, Yu H (2024) A novel fuzzy algorithm for assembly precision management. Appl Math Modell 135:790–806
27. Davidson JK, Mujezinović A, Shah JJ (2002) A new mathematical model for geometric tolerances as applied to round faces. J Mech Des 124(4):609–622
28. Mujezinović A, Davidson JK, Shah JJ (2004) A new mathematical model for geometric tolerances as applied to polygonal faces. J Mech Des 126(3):504–518
29. Giordano M, Duret D (1993) Clearance space and deviation space: application to three-dimensional chain of dimensions and positions. Proc CIRP CAT, Cachan, France
30. Teissandier D, Couétard Y, Gérard A (1999) A computer aided tolerancing model: proportioned assembly clearance volume. Comput Aided Des 31(13):805–817
31. Pierre L, Anselmetti B (2015) Comparison of analysis line and polytopes methods to determine the result of a tolerance chain. ASME J Comput Inf Sci Eng 15:021007
32. Xu S, Keyser J (2016) Statistical geometric computation on tolerances for dimensioning. Comput Aided Des 70:193–201
33. Anwer N, Schleich B, Mathieu L, Wartzack S (2014) From solid modelling to skin model shapes: shifting paradigms in computer-aided tolerancing. CIRP Ann Manuf Technol 63(1):137–140
34. Chan Q, Zhenyu L, Xiang P, Guifang D, Jianrong T (2015) Realistic geometry based feature modeling of complex part and its application in assembly quality analysis. ASME J Comput Inf Sci Eng 15:041007
35. Schleich B, Wartzack S (2018) Novel approaches for the assembly simulation of rigid skin model shapes in tolerance analysis. Comput Aided Des 101:1–11
36. Yan X, Ballu A (2018) Tolerance analysis using skin model shapes and linear complementarity conditions. J Manuf Sys 48:140–156
37. Bjørke Ø (1989) Computer-aided tolerancing. ASME Press, New York
38. Skowronski VJ, Turner JU (1996) Estimating gradients for statistical tolerance systems. Comput Aided Des 28:933–941
39. Chongying G, Jianhua L, Ke J (2016) Efficient statistical analysis of geometric tolerances using unified error distribution and an analytical variation model. Int J Adv Manuf Technol 84:347–360
40. Zhu H, Zhou X, Li H (2016) A novel tolerance analysis for mechanical assemblies based on convex method and non-probabilistic set theory. Int J Adv Manuf Technol 83:1649–1657
41. Cao Y, Yan H, Liu T, Yang J (2016) Application of quasi-Monte Carlo method based on good point set in tolerance analysis. ASME J Comput Inf Sci Eng 16:021008
42. Zhou C, Liu Z, Qiu C, Tan J (2021) A quasi-Monte Carlo statistical three-dimensional tolerance analysis method of products based on edge sampling. Assem Autom 41(4):501–513
43. Stuppy J, Meerkamm H (2009) Tolerance analysis of a crank mechanism by taking into account different kinds of deviation. Proc CIRP-CAT Conf, Annecy, France
44. Walter M, Sprüngel T, Wartzack S (2013) Tolerance analysis of systems in motion taking into account interactions between deviations. Proc IMech E Part B: J Eng Manuf 227:709–719
45. Ziegler P, Wartzack S (2015) A statistical method to identify main contributing tolerances in assemblability studies based on convex hull techniques. J Zhejiang Univ Sci A: Appl Phys Eng 16(5):361–370
46. Chitale AN, Davidson JK, Shah JJ (2019) Statistical tolerance analysis with sensitivities established from Tolerance-maps and deviation spaces. ASME J Comput Inf Sci Eng 19:041002
47. Schleich B, Wartzack S (2018) An approach to the sensitivity analysis in variation simulations considering form deviations. Procedia CIRP 75:273–278
48. Wan Din WI, Robinson TT, Armstrong CG, Jackson R (2016) Using CAD parameter sensitivities for stack-up tolerance allocation. Int J Interact Des Manuf 10:139–151
49. Armillotta A (2014) A static analogy for 2D tolerance analysis. Assem Autom 34(2):182–191
50. Armillotta A (2023) Tolerance analysis by static analogy on 2D assemblies with fits and fasteners. Int J Adv Manuf Technol 127(1/2):507–525
51. Armillotta A (2015) Force analysis as a support to computer-aided tolerancing of planar linkages. Mech Mach Theory 93:11–25
52. Wittwer JW, Chase KW, Howell LL (2004) The direct linearization method applied to position error in kinematic linkages. Mech Mach Theory. https://doi.org/10.1016/j.mechmachtheory.2004.01.001
53. Leishman RC, Chase KW (2010) Direct linearization method kinematic variation analysis. ASME Trans J Mech Des 132:071003
54. Liu SC, Hu SJ (1997) Variation simulation for deformable sheet metal assemblies using finite element methods. Trans ASME J Manuf Sci Eng 119:368–374
55. Camelio JA, Hu SJ, Marin SP (2004) Compliant assembly variation analysis using component geometric covariance. ASME J Manuf Sci Eng 126:355–360
56. Lindau B, Lindkvist L, Andersson A, Söderberg R (2013) Statistical shape modeling in virtual assembly using PCA-technique. J Manuf Syst 32:456–463
57. Söderberg R, Wärmefjord K, Carlson JS, Lindkvist L (2017) Toward a digital twin for real-time geometry assurance in individualized production. CIRP Ann Manuf Technol 66:137–140
58. Armillotta A (2024) Solving basic problems of compliant tolerance analysis by static analogy. Int J Manuf Technol 30:4325–4340
59. Shi Z (1997) Synthesis of mechanical error in spatial linkages based on reliability concept. Mech Mach Theory 32(2):255–259
60. Joskowicz L, Sacks E, Srinivasan V (1997) Kinematic tolerance analysis. Comput Aided Des 29(2):147–157
61. Sachs E, Joskowicz L (1997) Parametric kinematic tolerance analysis of planar mechanisms. Comput Aided Des 29(5):333–342
62. Kyung MH, Sacks E (2003) Nonlinear kinematic tolerance analysis of planar mechanical systems. Comput Aided Des 35:901–911
63. Ostrovsky-Berman Y, Joskowicz L (2005) Relative positioning of planar parts in toleranced assemblies. Comput Aided Des Appl 2:675–684
64. Tsai MJ, Lai TH (2004) Kinematic sensitivity analysis of linkage with joint clearance based on transmission quality. Mech Mach Theory 39:1189–1206
65. Chang WT, Wu LI (2013) Tolerance analysis and synthesis of cam-modulated linkages. Math Comput Model 57:641–660
66. Kumaraswamy U, Shunmugam MS, Sujatha S (2013) A unified framework for tolerance analysis of planar and spatial mechanisms using screw theory. Mech Mach Theory 69:168–184
67. Katam R, Pasupuleti VDK, Kalapatapu P (2023) Innov Infrastruct Solut 8:248
68. Van der Auweraer H, Peeters B (2003) Sensors and systems for structural health monitoring. J Struct Contr 10:117–125
69. Sony S, Laventure S, Sadhu A (2018) A literature review of next-generation smart sensing technology in structural health monitoring. Struct Contr Health Monit 26:e2321
70. Ferreira PM, Machado MA, Carvalho MS, Vidal C (2022) Embedded sensors for structural health monitoring: methodologies and applications review. Sensors 22:8320
71. Mendrok K, Maj W (2012) Application of the modal filtration to the damage detection in truss structure. Diagnostyka Appl Struct Health Usage Cond Monitor 4:31.37
72. Kolakowski P, Szelazek J, Sekula K, Swiercz A, Mizerski K, Gutkiewicz (2011) Structural health monitoring of a railway truss bridge using vibration-based and ultrasonic methods. Smart Mater Struct 20:035016
73. Li J, Hao H (2016) Health monitoring of joint conditions in steel truss bridges with relative displacement sensors. Measurement 88:360–371

74. Park HS, Sun S, Choi SW, Kim Y (2013) Wireless laser range finder system for vertical displacement monitoring of mega-trusses during construction. Sensors 13:5796–5813
75. An Y, Li B, Ou J (2013) An algorithm for damage localization in steel truss structures: numerical simulation and experimental validation. J Intell Mater Syst Struct 24(14):1683–1698
76. Ye XW, Dong CZ, Liu T (2016) A review of machine vision-based structural health monitoring: methodologies and applications. J Sens. https://doi.org/10.1155/2016/7103039
77. Dong CZ, Catbas FN (2021) A review of computer vision-based structural health monitoring at local and global levels. Struct Health Monit 20(2):692–743
78. Feng D, Feng MQ (2017) Experimental validation of cost-effective vision-based structural ealth monitoring. Mech Syst Signal Process 88:199–211
79. Feng D, Feng MQ (2018) Computer vision for SHM of civil infrastructure: from dynamic response measurement to damage detection – a review. Eng Struct 156:115–117
80. Kohut P. Holak K, Uhl T, Ortyl L, Owerko T, Kuras P, Kocierz R. Struct Health Monotir 12(5–6):411–429
81. Xu Y, Brownjohn JMW (2018) Review of machine-vision based methodologies for displacement measurement in civil structures. J Civil Struct Health Monit 8:91–110
82. Spencer BF, Hoskere V, Narazaki Y (2019) Advances in computer vision-based civil infrastructure inspection and monitoring. Eng 5:199–222
83. Lee JJ, Shinozuka M (2006) Real-time displacement measurement of a flexible bridge using digital image processing techniques. Exp Mech 46:105–114
84. Fukuda Y, Feng MQ, Shinozuka M (2010) Cost-effective vision-based system for monitoring dynamic response of civil engineering structures. Struct Contr Health Monit 17:918–936
85. Sladek J, Ostrowska K, Hohut P, Holak K, Gaska A, Uhl T (2013) Development of a vision based deflection measurement system and its accuracy assessment. Measurement 46:1237–1249
86. Almeida Santos C, Oliveira Costa C, Batista J (2016) A vision-based system for measuring the displacements of large structures: simultaneous adaptive calibration and full motion estimation. Mech Sys Signal Proc 72–73:678–694
87. Tibaduiza Burgos DA, Gomez Vargas RC, Pedraza C, Agis D, Pozo F (2020) Damage identification in structural health monitoring: a brief review from its implementation to the use of data-driven applications. Sensors. https://doi.org/10.3390/s20030733
88. Carden EP, Fanning P (2004) Vibration based condition monitoring: a review. Struct Health Monit 3(4):355–377
89. Fan W, Qiao P (2011) Vibration-based damage identification methods: a review and comparative study. Struct Health Monit 10(1):83–111
90. Guan H, Karbhari VM (2008) Improved damage detection method based on element modal strain damage index using sparse measurement. J Sound Vibr 309:465–494
91. Gawronski W, Sawicki JT (2000) Structural damage detection using modal norms. J Sound Vibr 229(1):194–198
92. Deraemaeker A, Preumont A (2006) Vibration based damage detection using large array sensors and spatial filters. Mech Sye Signal Proc 20:1615–1630
93. Patsias S, Staszewski WJ (2002) Damage detection using optical measurements and wavelets. Struct Health Monit 1(1):5–22
94. Bureerat S, Pholdee N (2018) Inverse problem based differential evolution for efficient structural health monitoring of trusses. Appl Soft Comput 66:462–472
95. Hou J, Li Z, Zhang Q, Zhou R, Jankowski L (2019) Optimal placement of virtual masses for structural damage identification. Sensors 19:340
96. Kim B, Min C, Kim H, Cho S, Oh J, Ha SH, Yi JH (2019) Structural health monitoring with sensor data and cosine similarity for multi-damages. Sensors (Basel) 19:3047
97. El-Ouafi Bahlous S, Abdelghani M, Smaoui H, El-Borgi S (2007) A modal filtering and statistical approach for damage detection and diagnosis in structures using ambient vibrations measurements. J Vibr Contr 13(3):281–308
98. Enshaeian A, Ghahremani B, Rizzo P (2024) Structural health moitoring of a lenticular truss bridge: a comprehensive study. Struct Health Monit 23(6):3615–3639
99. Markogiannaki O, Arailopoulos A, Giagopoulos D, Papadimitriou C (2023) Vibration-based damage localization and quantification framework of large-scale truss structures. Struct Health Monit 22(2):1376–1398
100. Parisi F, Mangini AM, Fanti MP, Adam JM (2022) Automated location of steel truss bridge damage using machine learning and raw strain sensor data. Autom Construct 138:104249
101. Guyan RJ (1965) Reduction of stiffness and mass matrices. AIAA J 3(2):380
102. Duarte Moura Neto F, da Silva Neto J (2013) An introduction to inverse problems with applications. Springer, Berlin
103. Cady F (2017) The data science handbook. Wiley, Hoboken NJ